Fate of Electromagnetic Field on the Cracking of PSR J1614-2230 in Quadratic Regime

M. Azam[1] *, S. A. Mardan[2] †and M. A. Rehman[2] ‡

[1] Division of Science and Technology, University of Education,
Township Campus, Lahore-54590, Pakistan.
[2] Department of Mathematics,
University of the Management and Technology,
C-II, Johar Town, Lahore-54590, Pakistan.

Abstract

In this paper, we study the cracking of compact object PSR J1614-2230 in quadratic regime with electromagnetic field. For this purpose, we develop a general formalism to determine the cracking of charged compact objects. We apply local density perturbations to hydrostatic equilibrium equation as well as physical variables involve in the model. We plot the force distribution function against radius of the star with different parametric values of model both with and without charge. It is found that PSR J1614-2230 remains stable (no cracking) corresponding to different values of parameters when charge is zero, while it exhibit cracking (unstable) when charge is introduced. We conclude that stability region increases as amount of charge increases.

Keywords: Self-gravitating objects; Cracking; Density perturbations; Electromagnetic field.
PACS: 04.20.-q; 04.40.Dg; 04.50.Gh.

*azam.math@ue.edu.pk
†syedalimardanazmi@yahoo.com
‡aziz3037@yahoo.com

1 Introduction

Self-gravitating compact objects (CO) like neutron stars, white dwarfs, millisecond pulsars, and so forth, belongs to a distinguish class of those celestial bodies whose study become very significant in novel astrophysical research. It is evident that when a star or system of stars burns out all its nuclear fuel, its remnants can have one of three possibilities: white dwarfs, neutron stars and black holes. The stability of stellar remnants plays a key role in general relativity (GR) as well as modified relativistic theories [1]. The occurrence of gravitational collapse may be as a result of cooling of gaseous material, change in anisotropy, fluctuation of gravitational waves and variation of electromagnetic field of CO [2]. Therefore, such phenomena stimulate our interest to study the stability regions of these self-gravitating CO.

Astronomical objects are not physically viable, if they are unstable towards perturbations. Therefore, it is important to check the stability of these objects. In this context, Bondi [3] initially developed hydrostatic equilibrium equation to examine the stability of self-gravitating spheres. Chandrasekhar [4] calculated the principle value, i.e., $\frac{4}{3}$ to determine the dynamical instability of sphere filled with perfect fluid in GR. Herrera [5] presented the technique of cracking to discuss gravitational collapse of self-gravitating spherical CO. This technique interprets the behavior of inner fluid distribution of CO just after equilibrium state is disturbed. Cracking takes place in CO when radial forces changes its sign from positive to negative and vice versa [6]. Several authors [7]-[10] studied non-local effects of cracking through radial sound speed velocities and Raychaudhuri equation for spherically symmetric CO. Gonzalez [11, 12] presented the idea of local density perturbation (DP) to discussed the idea of cracking for relativistic spheres.

To study the effect of charge on the physical properties of stars is an important subject in GR. In this scenario, Bonnor [13, 14] explored the effect of charge on spherically symmetric CO and found that electric repulsion can halt the gravitational collapse. Bondi [15] used local Minkowski coordinates to described the contraction of radiating isotropic spherical symmetry. The main hindrance in astrophysics and GR is to develop stable mathematical models which describes the characteristic of charged spherical CO. Bekenstein [16] presented the idea of gravitational collapse in charged CO. Ray et al. [17] found the maximum amount of charge, (i.e., approximately 10^{20} coulomb), needed for CO to be in equilibrium configuration. Some authors [18, 19] studied the impact of charge on gravitational collapse of celestial objects

and analyzed the tendency of self-gravitating systems to produce charged black holes or naked singularities. Sharif and Azam [20, 21] studied the stability of spherical and cylindrical symmetric objects under the influence of electromagnetic field.

Demorest et al. [22] used the Green Bank Telescope at the National Radio Astronomy Observatory to analyze the system of stars by means of Shapiro delay (SD) and presented the observed values of different physical parameters for PSR J1614-2230. These physical parameters like ecliptic longitude, ecliptic latitude, parallax pulsar spin, pulsar spin period, orbital period, companion mass, radius, and so forth are recorded with very high precision by SD for PSR J1614-2230. The availability of very accurate parametric values made PSR J1614-2230 extremely important for modern research in GR. Neutron stars are made of the most dense material exist in this universe. Tauris et al. [23] developed mathematical model of PSR J1614-2230 and provided the possible variation of masses to show that PSR J1614-2230 was born more massive as compared to any discovered neutron star. Lin et al. [24] used stellar evaluation code "MESA" to describe the relationship between PSR J1614-2230 and its stellar companion. This discovery of high massive neutron star has extensive consequences on the equation of state (EoS) of matter with high densities. The relationship between physical parameters become more complicated as linear EoS is replaced by nonlinear EoS. In this work, we apply the concept of cracking to self-gravitating CO in the presence of electromagnetic field in quadratic regime. Here, we take local density perturbation (DP) which is different from constant DP presented by Herrera [5]. We applied this technique to the model of charged compact objects with quadratic EoS presented by Takisa et al. [25] and determine the cracking of newly discovered PSR J1614-2230 with electromagnetic field. Recently, we have investigated the cracking of some compact objects with and without electromagnetic field in linear regime [26].

This paper is arranged as follows. Section **2** deals with Einsten-Maxwell field and TolmanOppenheimerVolkoff (TOV) equations corresponding to anisotropic fluid. We present the general formalism to determine the cracking of charged CO with local DP in the quadratic regime in section **3**. Section **4** investigate stable and unstable regions of compact star PSR J1614-2230. In the last section, we conclude our results.

2 Einstein-Maxwell Field and TolmanOppenheimerVolkoff Equations

We consider the line element for a static spherically symmetric space time in curvature coordinates given by

$$ds^2 = -e^{2\nu}dt^2 + e^{2\lambda}dr^2 + r^2(d\theta^2 + \sin^2\theta d\phi^2), \tag{1}$$

where $0 \leq \theta \leq \pi$, $0 \leq \phi < 2\pi$ and $\nu = \nu(r)$, $\lambda = \lambda(r)$ are gravitational potentials. The Maxwell's equations are defined as

$$F_{ab;c} + F_{bc;a} + F_{ca;b} = 0, \tag{2}$$

$$F^{ab}_{;b} = 4\pi J^a, \quad E_{ab} = F_{ac}F^c_b - \frac{1}{4}g_{ab}F_{cd}F^{cd}, \tag{3}$$

where F^{ab} is the electromagnetic field tensor, J is the four current density and E_{ab} is the electromagnetic energy-momentum tensor [27]. The skew-symmetric electromagnetic field tensor can be decomposed as

$$F^{ab} = \begin{bmatrix} 0 & E_x & E_y & E_z \\ -E_x & 0 & B_z & B_y \\ -E_y & -B_z & 0 & B_x \\ -E_z & -B_y & -B_x & 0 \end{bmatrix}, \tag{4}$$

where $\mathbf{E} = (E_x, E_y, E_z)$ is the electric field and $\mathbf{B} = (B_x, B_y, B_z)$ is the magnetic field. The electromagnetic field tensor and four current density can be defined as

$$F_{ab} = A_{b,a} - A_{a,b}, \quad J^a = \sigma u^a, \tag{5}$$

where A and σ are the four potential and proper charge density and $u^a = e^{-\nu}\delta^a_0$ is four vector velocity of the fluid. The four potential is defined as

$$A_a = (\phi(r), 0, 0, 0). \tag{6}$$

Using this in above equation, it yields

$$F_{01} = -\phi'(r), \tag{7}$$

which can also be written as

$$F^{01} = e^{-2(\nu+\lambda)}\phi'(r) = e^{-(\nu+\lambda)}E(r), \tag{8}$$

4

where, we have used $E(r) = e^{-(\nu+\lambda)}\phi'(r)$. The total energy-momentum tensor corresponding to charged anisotropic fluid sphere is defined by [27]

$$T_{ab} = diag(-\rho - \frac{E^2}{2}, P_r - \frac{E^2}{2}, P_t + \frac{E^2}{2}, P_t + \frac{E^2}{2}). \qquad (9)$$

The terms E, ρ, P_r and P_t are electromagnetic field, energy density, radial and tangential pressure respectively.

The synergies of electromagnetic field and matter are governed by system of field equations. These synergies of spherically symmetric metric corresponds to Einstein-Maxwell field equations given by

$$G_{ab} = \kappa T_{ab} = \kappa(M_{ab} + E_{ab}) \qquad (10)$$

where M_{ab} is the energy momentum tensor for the fluid inside the star and $E_{ab} = F_{ac}F_b^c - \frac{1}{4}g_{ab}F_{cd}F^{cd}$ is electromagnetic field tensor. The non-zero components of Einstein-Maxwell field equations corresponding to Eqs.(1) and (9) are given as follows

$$1 + e^{-2\lambda}(2r\lambda' - 1) = 8\pi r^2 \rho + r^2 \frac{E^2}{2}, \qquad (11)$$

$$1 - e^{-2\lambda}(2r\nu' + 1) = -8\pi r^2 P_r + r^2 \frac{E^2}{2}, \qquad (12)$$

$$e^{-2\lambda}(\lambda'r - \nu'r - \nu''r^2 + \nu'\lambda'r^2 - (\nu')^2 r^2) = -8\pi r^2 P_t - r^2 \frac{E^2}{2}, \qquad (13)$$

$$r^2 \sigma = e^{-\lambda}(r^2 E)', \qquad (14)$$

where "$\prime$" denotes the differentiation with respect to r.

It is clear that the choice of EoS of fluid inside the star plays a key role for its physical significance. Thus, a star is physically acceptable, if it satisfy the barotropic EoS $P_r = P_r(\rho)$. In this work, we have used the quadratic EoS to explore the stability of PSR J1614-2230. The quadratic EoS is given by [25]

$$P_r = \gamma\rho^2 + \alpha\rho - \beta, \qquad (15)$$

where γ, α and β are constants and are constrained by ($\rho \leq \frac{1+\alpha}{2\gamma}$) and $\beta = \alpha\rho_\varepsilon$, where $\rho_\varepsilon = 0.5 \times 10^{15} g/cm^3$ gives the density at the boundary surface of sphere. It is interesting to note that this equation reduce to linear EoS, when $\gamma = 0$ [25].

5

Solving Eqs.(11)-(13) simultaneously, we obtain hydrostatic equilibrium equation (TOV) for anisotropic charged fluid

$$\frac{dP_r}{dr} = \frac{2(P_t - P_r)}{r} - (\rho + P_r)\nu' + \frac{E}{8\pi r^2}(r^2 E)', \tag{16}$$

which shows that gradient of pressure is effected by charge and anisotropy of fluid. Using the relation $e^{-2\lambda(r)} = 1 - 2M/r + Q^2/r^2$ in the above equation [27], it yields

$$\Omega = -\frac{dP_r}{dr} + \frac{2(P_t - P_r)}{r} + (\rho + P_r)\frac{-\frac{4M}{r} + 4r^2 E^2 - 8\pi r^2 P_r}{4r(1 - \frac{2M}{r} + r^2 E^2)} + \frac{(r^2 E)' E}{4\pi r^2} = 0, \tag{17}$$

where the mass function with $Q = r^2 E$ is defined as

$$M = 4\pi \int_0^r (\rho(x) + \frac{E^2}{8\pi})x^2 dx. \tag{18}$$

3 Effect of Local Density Perturbation

In this section, we perturb the equilibrium configuration of charged CO through local DP ($\delta\rho$). Eq.(17) depicts that cracking take place in interior of spherical CO when equilibrium state is interrupted due to change in sign of perturb force i.e., $\delta\Omega < 0 \to \delta\Omega > 0$ and vice-versa. We apply the local DP to Eq.(17) and all the physical variables like mass, radial and tangential pressure, electromagnetic field and their derivatives involve in Eq.(17), given by

$$P_r(\rho + \delta\rho) = P_r(\rho) + \frac{dP_r}{d\rho}\delta\rho, \tag{19}$$

$$\frac{dP_r}{dr}(\rho + \delta\rho) = \frac{dP_r}{dr}(\rho) + \left[\frac{d}{dr}\left(\frac{dP_r}{d\rho}\right) + \frac{dP_r}{d\rho}\frac{d^2\rho}{dr^2}\frac{1}{\frac{d\rho}{dr}}\right]\delta\rho, \tag{20}$$

$$P_t(\rho + \delta\rho) = P_t(\rho) + \frac{dP_t}{d\rho}\delta\rho, \tag{21}$$

$$M(\rho + \delta\rho) = M(\rho) + \frac{dM}{d\rho}\delta\rho, \tag{22}$$

$$E(\rho + \delta\rho) = E(\rho) + \frac{E'}{\rho'}\delta\rho, \tag{23}$$

$$E'(\rho + \delta\rho) = E'(\rho) + \frac{E''}{\rho'}\delta\rho. \tag{24}$$

6

The radial sound speed v_r^2 and tangential sound speed v_t^2 are define as

$$v_r^2 = \frac{dP_r}{d\rho} \quad \& \quad v_t^2 = \frac{dP_t}{d\rho}. \tag{25}$$

The perturb form of Eq.(17) is given by

$$\Omega = \Omega_0(\rho, P_r, P_r', P_t, M, E, E') + \delta\Omega, \tag{26}$$

where

$$\delta\Omega = \frac{\partial\Omega}{\partial\rho}\delta\rho + \frac{\partial\Omega}{\partial P_r}\delta P_r + \frac{\partial\Omega}{\partial P_r'}\delta P_r' + \frac{\partial\Omega}{\partial P_t}\delta P_t + \frac{\partial\Omega}{\partial M}\delta M + \frac{\partial\Omega}{\partial E}\delta E + \frac{\partial\Omega}{\partial E'}\delta E', \tag{27}$$

which can also be written as

$$
\begin{aligned}
\frac{\delta\Omega}{\delta\rho} &= \frac{\partial\Omega}{\partial\rho} + \frac{\partial\Omega}{\partial P_r}v_r^2 + \frac{\partial\Omega}{\partial P_r'}(v_r^{2'} + v_r^2\rho''(\rho')^{-1}) + \frac{\partial\Omega}{\partial P_t}v_t^{2'} \\
&\quad + \frac{4\pi r^2}{\rho'}\frac{\partial\Omega}{\partial M}(\rho + \frac{E^2}{2}) + \frac{\partial\Omega}{\partial E}\frac{E'}{\rho\prime} + \frac{\partial\Omega}{\partial E'}\frac{E''}{\rho\prime}.
\end{aligned}
\tag{28}
$$

This is the fundamental equation used to determine the effects of local DP on the cracking of charged anisotropic fluid. We will plot the force distribution function $\frac{\delta\Omega}{\delta\rho}$ against radius "r" of the star for different values of the parameters involve in the model. Using Eq.(17), the derivatives involve in the above equation are given as follows

$$\frac{\partial\Omega}{\partial\rho} = \frac{-4M - 16\pi r^3 P_r + 3r^3 E^2}{4r^2 - 8Mr + 4r^4 E^2}, \tag{29}$$

$$\frac{\partial\Omega}{\partial M} = -\frac{(\rho + P_r)(4r^2 - 16\pi r^4 P_r - 2r^4 E^2)}{(2r^2 - 4Mr + 2r^4 E^2)^2}, \tag{30}$$

$$\frac{\partial\Omega}{\partial P_r} = -\frac{2}{r} - \frac{2M + 16\pi r^3 P_r + 8\pi r^3\rho - r^3 E^2}{2r^2 - 4Mr + 2r^4 E^2} + \frac{r^2 E^2}{4r - 8M + 4r^3 E^2}, \tag{31}$$

$$\frac{\partial\Omega}{\partial P_t} = \frac{2}{r}, \quad \frac{\partial\Omega}{\partial P_r'} = -1, \tag{32}$$

$$\frac{\partial\Omega}{\partial E} = -\frac{(\rho + P_r)(r^2 E)(3r - 10M + 6r^3 E^2 - 6\pi r^3 P_r)}{2(r - 2M + r^3 E^3)^2} + \frac{2 + rE'}{8\pi r}, \tag{33}$$

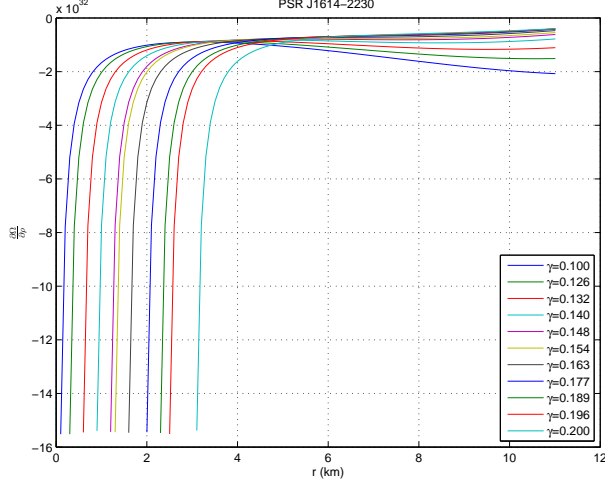$$\frac{\partial\Omega}{\partial E'} = \frac{E}{8\pi}. \tag{34}$$

Figure 1: Plots shows that there is no cracking, i.e., the PSR J1614-2230 remains stable for different values of the parameters involved in the model given in Table 1, when $E = 0$ in quadratic regime.

4   Cracking of PSR J1614-2230

Here, we apply the formalism developed in the above section to investigate the cracking of charged objects for the model given by Takisa et al. [25]. This model is consistent with the physical features of observed objects and its connection can be made with PSR J1614-2230 for particular values of parameters given in [25]. The analysis of Takisa was seems to be consistent with observational objects such as Vela X-1, Cen X-3, SMC X-1, PSR J1903-327 and PSR J1614-2230. But our focus in this analysis is the particular object PSR J1614-2230 because its mass and radius has been measured with great accuracy. The model is defined by following equations

$$
\begin{aligned}
M(r) &= \frac{r^3 \left(4\,a - 4\,b\right)}{8\left(a\,r^2 + 1\right)} + \frac{5\,s\,\arctan\sqrt{a\,r^2}}{8\,a^{\frac{3}{2}}} \\
&\quad - \frac{r\,s\left(-2\,a^2\,r^4 + 10\,a\,r^2 + 15\right)}{24\,a\left(r^2 + a + 1\right)},
\end{aligned} \tag{35}
$$

$$
\rho = \frac{\left(2\,a - 2\,b\right)\left(a\,r^2 + 3\right) - a^2\,r^4\,s}{16\,\pi\left(a\,r^2 + 1\right)^2}, \tag{36}
$$

8
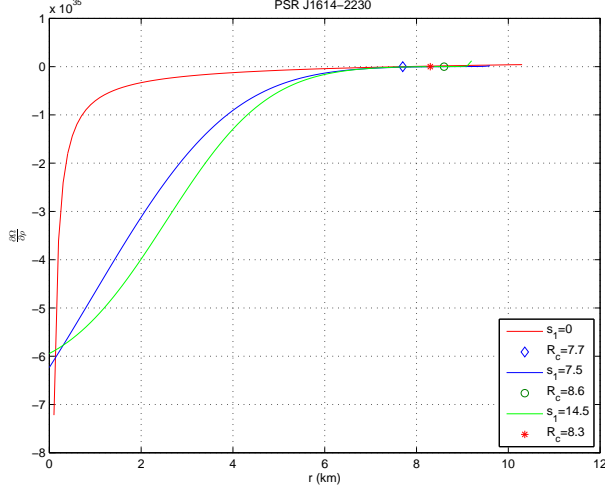
Figure 2: Cracking of PSR J1614-2230 with $\gamma = 0.0$, $\alpha = 0.99$ and $s_1 = 0, 7.5, 14.5$.

$$
\begin{aligned}
P_r &= \frac{\gamma \left[(2\,a - 2\,b)\,(a\,r^2 + 3) - a^2\,r^4\,s\right]^2}{256\,\pi^2\,(a\,r^2 + 1)^4} \\
&+ \frac{\alpha \left[(2\,a - 2\,b)\,(a\,r^2 + 3) - a^2\,r^4\,s\right]}{16\,\pi\,(a\,r^2 + 1)^2} - \beta,
\end{aligned}
\tag{37}
$$

$$
P_t = P_r + \Delta,
\tag{38}
$$

where

$$
\begin{aligned}
8\pi\Delta &= \frac{4\,r^2\,(b\,r^2 + 1)}{a\,r^2 + 1} \left(\frac{F''}{2\,r^2} - \frac{F'}{2\,r^3} + \frac{F'^2}{4\,r^2} + \frac{b^2\,n\,(n-1)}{(b\,r^2 + 1)^2} \right. \\
&\left. + \frac{a^2\,t\,(t-1)}{(a\,r^2 + 1)^2} + \frac{F'\,b\,n}{r\,(b\,r^2 + 1)} + \frac{F'\,a\,t}{r\,(a\,r^2 + 1)} + \frac{2\,a\,b\,n\,t}{(a\,r^2 + 1)\,(b\,r^2 + 1)} \right) \\
&\left(\frac{4\,b\,r^2 + 4}{a\,r^2 + 1} - \frac{r^2\,(2\,a - 2\,b)}{(a\,r^2 + 1)^2} \right) \left(\frac{F'}{2\,r} + \frac{b\,n}{b\,r^2 + 1} + \frac{a\,t}{a\,r^2 + 1} \right) \\
&- \frac{2\,a - 2\,b - 16\,\pi\,\beta\,(a\,r^2 + 1)^2 + a^2\,r^2\,s}{2\,(a\,r^2 + 1)^2} - \frac{\alpha\,((2\,a - 2\,b)\,(a\,r^2 + 3) + a^2\,r^2\,s)}{2\,(a\,r^2 + 1)^2} \\
&- \frac{\gamma\,((a - b)\,(a\,r^2 + 3) - a^2\,r^4\,s)}{64\,\pi\,(a\,r^2 + 1)^2},
\end{aligned}
\tag{39}
$$

9

and

$$t = \frac{\alpha}{2} + \gamma \left(2\,a - 2\,b\right)^2 \left(\frac{b}{(a-b)^2} - \frac{b^2}{(a-b)^3} + \frac{1}{4}\right) + \frac{s\,(\alpha+1)}{8\,a - 8\,b}$$

$$+ \frac{\gamma\,s\,(2\,b^3\,(2\,a - 1) + (a - b)\,(a + b + 2\,s\,(a - b)) - 6\,a\,b^2)}{8\,(a - b)^3}, \quad (40)$$

$$n = \frac{\beta\,(a - b)}{4\,b^2} + \gamma\,(2\,a - 2\,b)^2 \left(\frac{b}{(a-b)^2} - \frac{b^2}{(a-b)^3} + \frac{1}{4}\right)$$

$$+ \frac{2\,\alpha\,(a - b)}{4\,a - 4\,b} + \frac{\gamma\,s\,(2\,b\,(2\,a^3\,b - 6\,a^2\,b^2) - a^4\,(4\,b + s))}{16\,b^2\,(a - b)^3}$$

$$+ \frac{(a - b)\,(\alpha + 1)}{4\,b} - \frac{a^2\,s\,(\alpha + 1)}{8\,b^2\,(a - b)}, \quad (41)$$

$$E^2 = \frac{s a^2 r^4}{(1 + a r^2)^2}. \quad (42)$$

The radial and tangential sound speed velocities can be obtained from Eqs.(37) and (38) as

$$v_r^2 = \alpha + 2\,\gamma\,\rho, \quad (43)$$

and

$$v_t^2 = \left[\frac{2199023255552\gamma((2\,a - 2\,b)(3 + a r^2) - s a^2 r^4)((4\,a - 4\,b)a r - 4\,s a^2 r^3)}{2778046668940015(1 + a r^2)^4}\right.$$

$$- \frac{8796093022208\gamma((2\,a - 2\,b)(3 + a r^2) - s a^2 r^4)^2 a r}{2778046668940015(1 + a r^2)^5}$$

$$+ 1/16\,\frac{\alpha\,((4\,a - 4\,b)a r - 4\,s a^2 r^3)}{\pi\,(1 + a r^2)^2} - 1/4\,\frac{\alpha\,((2\,a - 2\,b)(3 + a r^2) - s a^2 r^4)a r}{\pi\,(1 + a r^2)^3}$$

$$+ \left\{r(1 + b r^2)\left(\frac{t(t - 1)a^2}{(1 + a r^2)^2} + 2\,\frac{t n a b}{(1 + a r^2)(1 + b r^2)} + \frac{t a F'}{r(1 + a r^2)}\right.\right.$$

$$+ \frac{b^2 n(n - 1)}{(1 + b r^2)^2} + \frac{n b F'}{r(1 + b r^2)} + 1/2\,\frac{F''}{r^2} - 1/2\,\frac{F'}{r^3} + 1/4\,\frac{F'^2}{r^2}\left.\right)(1 + a r^2)^{-1}$$
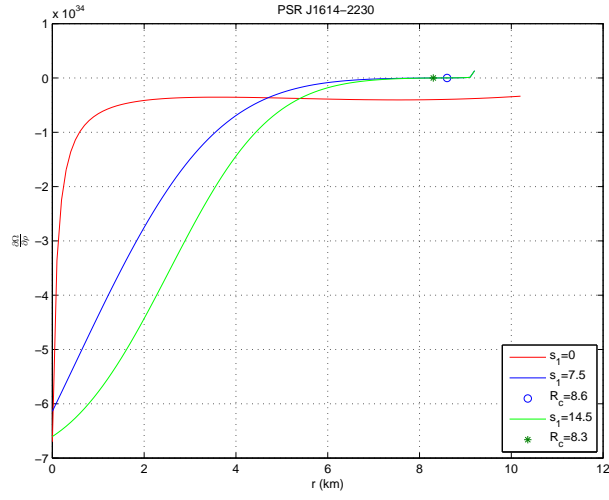
Figure 3: Cracking of PSR J1614-2230 with $\gamma = 0.140$, $\alpha = 0.33$ and $s_1 = 0, 7.5, 14.5$.
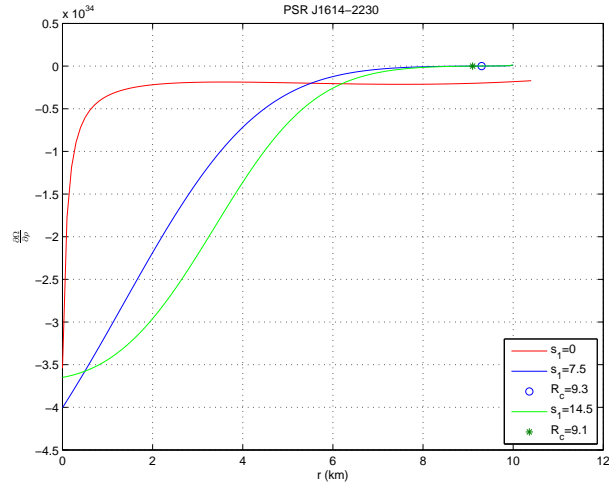

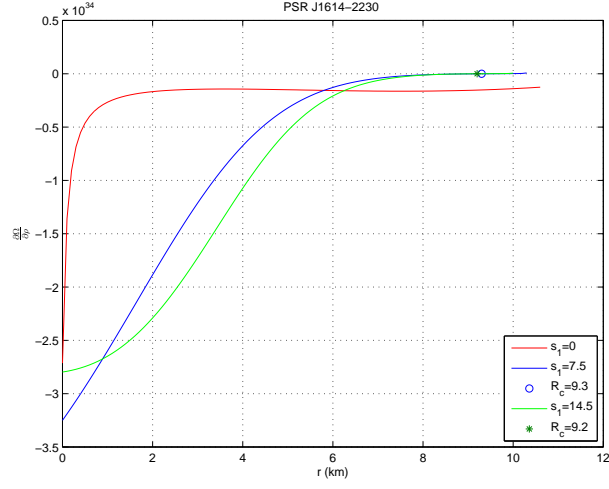Figure 4: Cracking of PSR J1614-2230 with $\gamma = 0.158$, $\alpha = 0.24$ and $s_1 = 0, 7.5, 14.5$.

11

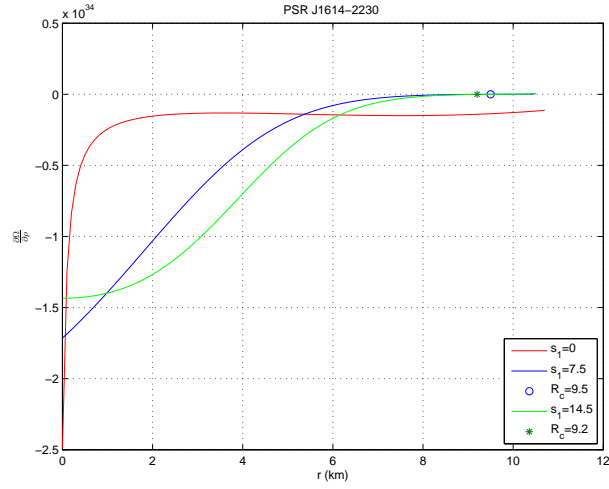Figure 5: Cracking of PSR J1614-2230 with $\gamma = 0.163$, $\alpha = 0.21$ and $s_1 = 0, 7.5, 14.5$.

Figure 6: Cracking of PSR J1614-2230 with $\gamma = 0.177$, $\alpha = 0.15$ and $s_1 = 0, 7.5, 14.5$.

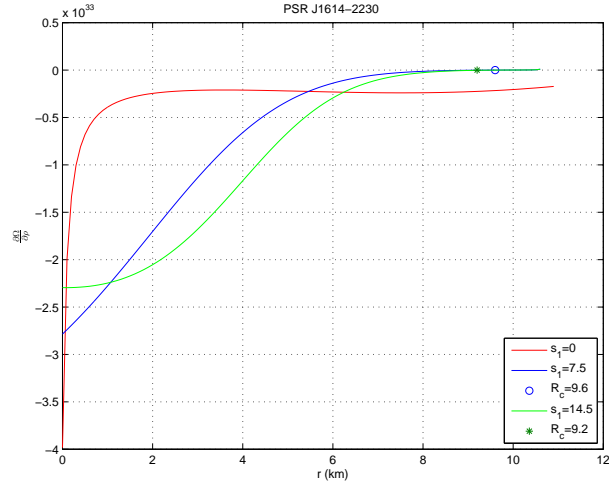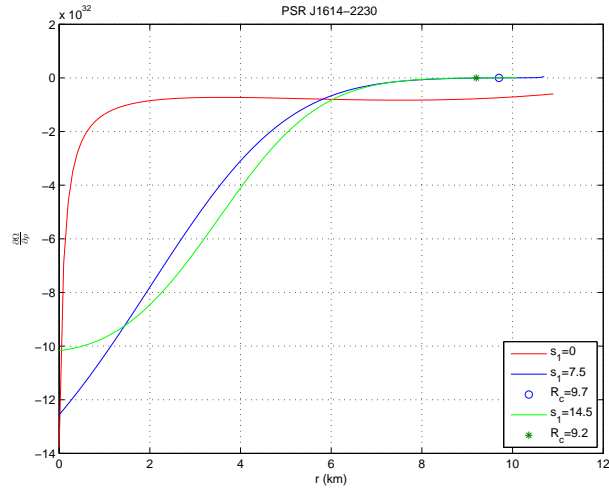Figure 7: Stability regions for $\gamma = 0.196$, $\alpha = 0.06$ and $s_1 = 0, 7.5, 14.5$

Figure 8: Stability regions for $\gamma = 0.200$, $\alpha = 0.04$ and $s_1 = 0, 7.5, 14.5$

13

$$+r^3 b\left(\frac{t(t-1)a^2}{(1+ar^2)^2} + 2\frac{tnab}{(1+ar^2)(1+br^2)} + \frac{taF'}{r(1+ar^2)}\right.$$

$$\left.+\frac{b^2 n(n-1)}{(1+br^2)^2} + \frac{nbF'}{r(1+br^2)} + 1/2\frac{F''}{r^2} - 1/2\frac{F'}{r^3} + 1/4\frac{F'^2}{r^2}\right)(1+ar^2)^{-1}$$

$$-r^3(1+br^2)\left(\frac{t(t-1)a^2}{(1+ar^2)^2} + 2\frac{tnab}{(1+ar^2)(1+br^2)} + \frac{taF'}{r(1+ar^2)}\right.$$

$$\left.+\frac{b^2 n(n-1)}{(1+br^2)^2} + \frac{nbF'}{r(1+br^2)} + 1/2\frac{F''}{r^2} - 1/2\frac{F'}{r^3} + 1/4\frac{F'^2}{r^2}\right)$$

$$a(1+ar^2)^{-2} + 1/2\,r^2(1+br^2)\left(-4\frac{t(t-1)a^3 r}{(1+ar^2)^3} - 4\frac{tna^2 br}{(1+ar^2)^2(1+br^2)}\right.$$

$$-4\frac{tnab^2 r}{(1+ar^2)(1+br^2)^2} - \frac{taF'}{r^2(1+ar^2)} - 2\frac{ta^2 F'}{(1+ar^2)^2} - 4\frac{b^3 n(n-1)r}{(1+br^2)^3}$$

$$\left.-\frac{nbF'}{r^2(1+br^2)} - 2\frac{b^2 nF'}{(1+br^2)^2} - \frac{F''}{r^3} + 3/2\frac{F'}{r^4} - 1/2\frac{F'^2}{r^3}\right)(1+ar^2)^{-1}$$

$$+1/8\left(\frac{(-4\,a + 4\,b)r}{(1+ar^2)^2} - \frac{(-8\,a + 8\,b)r^3 a}{(1+ar^2)^3} + 8\frac{br}{1+ar^2}\right.$$

$$\left.-\frac{(8 + 8\,br^2)ar}{(1+ar^2)^2}\right)\left(\frac{ta}{1+ar^2} + \frac{nb}{1+br^2} + 1/2\frac{F'}{r}\right)$$

$$+1/8\left(\frac{(-2\,a + 2\,b)r^2}{(1+ar^2)^2} + \frac{4 + 4\,br^2}{1+ar^2}\right)\left(-2\frac{ta^2 r}{(1+ar^2)^2} - 2\frac{b^2 nr}{(1+br^2)^2} - 1/2\frac{F'}{r^2}\right)$$

$$-\frac{1}{512}\frac{\gamma((2\,a - 2\,b)ar - 4\,sa^2 r^3)}{\pi\,(1+ar^2)^2} + \frac{1}{128}\frac{\gamma((a-b)(3+ar^2) - sa^2 r^4)ar}{\pi\,(1+ar^2)^3}$$

$$+1/8\frac{(4\,a - 4\,b + 2\,sa^2 r^2 - 32\,\pi\,\beta\,(1+ar^2)^2)ar}{(1+ar^2)^3}$$

$$\left.-1/16\frac{\alpha\,((4\,a - 4\,b)ar + 2\,sa^2 r)}{(1+ar^2)^2} + 1/4\frac{\alpha\,((2\,a - 2\,b)(3+ar^2) + sa^2 r^2)ar}{(1+ar^2)^3}\right\}\pi^{-1}\right]$$

$$\left(\frac{(1/4\,a - 1/4\,b)ar - 1/4\,sa^2 r^3}{\pi\,(1+ar^2)^2} - \frac{((1/2\,a - 1/2\,b)(3+ar^2) - 1/4\,sa^2 r^4)ar}{\pi\,(1+ar^2)^3}\right)^{-1}$$

14

$$-1/8 \, \frac{sa^2r - 32\,\pi\,\beta\,(1 + ar^2)ar}{(1 + ar^2)^2}. \tag{44}$$

Table 1: Stability of neutral PSR J1614-2230 when γ and b_1 are variable

γ	a_1	b_1	α	r(km)	R_c(km)
0.100	53.34	6.90	0.33	11.07	Stable
0.126	53.34	8.74	0.33	10.85	Stable
0.132	53.34	10.74	0.33	10.60	Stable
0.140	53.34	13.33	0.33	10.30	Stable
0.148	53.34	15.61	0.33	9.99	Stable
0.154	53.34	16.87	0.33	9.82	Stable
0.163	53.34	19.04	0.33	9.51	Stable
0.177	53.34	21.72	0.33	9.13	Stable
0.189	53.34	23.64	0.33	8.83	Stable
0.196	53.34	24.73	0.33	8.65	Stable
0.200	53.34	28.42	0.33	8.04	Stable

Table 2: Stability of PSR J1614-2230 when $s_1 = 0$ and α, γ are variable

γ	a_1	b_1	α	r(km)	R_c(km)
0.0	53.34	13.33	0.99	10.30	7.7
0.140	53.34	13.33	0.33	10.30	Stable
0.158	53.34	13.33	0.24	10.50	Stable
0.163	53.34	13.33	0.21	10.70	Stable
0.177	53.34	13.33	0.15	10.90	Stable
0.196	53.34	13.33	0.06	11.06	Stable
0.200	53.34	13.33	0.04	11.09	Stable

The constants a, b and s have dimension of length (L^{-2}) and chosen in such a way that the given system satisfy the following conditions

- energy density must remains positive before and after equilibrium state.

Table 3: Stability of PSR J1614-2230 when $s_1 = 7.5$ and α, γ are variable

γ	a_1	b_1	α	r(km)	R_c(km)
0.0	53.34	13.33	0.99	9.67	8.6
0.140	53.34	13.33	0.33	9.67	8.6
0.158	53.34	13.33	0.24	10.07	9.3
0.163	53.34	13.33	0.21	10.37	9.3
0.177	53.34	13.33	0.15	10.56	9.5
0.196	53.34	13.33	0.06	10.65	9.6
0.200	53.34	13.33	0.04	10.64	9.7

Table 4: Stability of PSR J1614-2230 when $s_1 = 14.5$ and α, γ are variable

γ	a_1	b_1	α	r(km)	R_c(km)
0.0	53.34	13.33	0.99	9.21	8.3
0.140	53.34	13.33	0.33	9.21	8.3
0.158	53.34	13.33	0.24	10.05	9.1
0.163	53.34	13.33	0.21	10.10	9.1
0.177	53.34	13.33	0.15	10.15	9.2
0.196	53.34	13.33	0.06	10.18	9.2
0.200	53.34	13.33	0.04	10.19	9.2

- radial pressure should be vanishes at the boundary of star.

- At the center of star i.e. $r = 0$, we have $P_r = P_t = \Delta = 0$.

- v_r^2 is constant in the quadratic regime.

- Across boundary of star, when $r = \varepsilon$, we have
$e^{-2\lambda} = 1 - 2M/\varepsilon + Q^2/\varepsilon^2$
$e^{-2\nu} = 1 - 2M/\varepsilon + Q^2/\varepsilon^2$

By considering above conditions, we have

$$\alpha = 0.33, \quad a = \frac{a_1}{\Re^2}, \quad b = \frac{b_1}{\Re^2}, \quad s = \frac{s_1}{\Re^2}$$

where $\Re$=43.245 km and the values given above are compatible with observational values given by Takisa et al. [25].

For the sake of regions (stable and unstable) of PSR J1614-2230, we have plotted force distribution function against radius of the star for different values of the parameters involve in the model shown in Figures **1-8**. We summarizes these results as follows:

- Figure **1** depicts that all curves do not change its sign with different values of γ and b_1 corresponding to Table **1**. Hence, we find that PSR J1614-2230 is stable in the absence of charge in quadratic regime and it is unstable in linear regime which is analogous to the results found in [26]. From Table **2**, it is clear that any variation in coefficients of quadratic EoS does not effect stability even radius of PSR J1614-2230 changes approximately to 4%.

- In Figure **2**, there are three curves corresponding to model parameters $\gamma = 0.0$, $\alpha = 0.99$ and charge $s_1 = 0$, 7.5, 14.5. It is noted that all three curves (red, blue and green) change its sign for charge parameter ($s_1 = 0$, 7.5, 14.5), respectively in the linear regime. This shows that PSR J1614-2230 is unstable in linear regime, where the symbols " $\diamond$ ", " o ", " $*$ " represents the cracking points (where curve changes its sign from negative to positive) corresponding to $s_1 = 0$, 7.5, 14.5, respectively. The cracking values $R_c = 7.7$, 8.6, 8.3 corresponds to $s_1 = 0$, 7.5, 14.5 (red, blue and green) are given in (Table **2,3,4**). In this case, our results are consisted with [26] in linear regime.

- Figures **3-8** represents the cracking of PSR J1614-2230 star for fixed values of parameters $\gamma = 0.140, 0.158, 0.163, 0.177, 0.196, 0.200$, $\alpha = 0.33, 0.24, 0.21, 0.15, 0.06, 0.04$ and charge $s_1 = 0.0, 7.5, 14.5$ in quadratic regime. We see that cracking take place for charge parameter $s_1 = 7.5$ and 14.5, which are indicated by the cracking points "o" and " $*$ " corresponding to blue and green curves, respectively. These cracking points (R_c) are given in Table **3-4**. However, in each case, the star remain stable, i.e., no cracking take place for $s_1 = 0$ in quadratic regime. Hence, PSR J1614-2230 exhibit cracking both in linear and quadratic regime when charge is present. From these illustrations, we conclude that as charge increases cracking points are slightly shifted towards center, which indicates that binding forces of CO become stronger and more mass is directed towards origin.

5 Conclusions and observations

We have applied the technique of cracking presented by Herrera [5] to charged anisotropic self-gravitating CO. The impact of local DP on the stability of inner fluid of star in the presence of charge is considered in the scenario of GR. It has been observed that cracking of CO takes place when the system leave its equilibrium state. The numerical value of R_c (cracking point) provides the stable/unstable region in the quadratic regime.

We have used the model of Takisa et al. [25] to investigate the cracking of PSR J1614-2230 with and without charge. Figure **1** represents the stability of celestial object PSR J1614-2230 in the absence of charge for different values of parameters γ and b_1 given in Table **1**. It is shown that PSR J1614-2230 remains stable, when quadratic EoS is considered in neutral case but it exhibited cracking with the inclusion of charge. Figure **2** has been plotted for $\gamma = 0.0$ and different values of α and charge $s_1 = 0$, 7.5, 14.5. It is shown that PSR J1614-2230 exhibit cracking in each case given by $R_c = 7.7, 8.6, 8.3$. For $s_1 = 0$, PSR J1614-2230 shows cracking which is consistent with our recent published work [26]. It is worth mentioned here that our results are analogous to [26], when $\gamma = 0$ (Linear Regime) in the presence of charge.

In figures **3-8**, we have given the comparison of stability region with different values of α, γ and charge parameter s_1. In these figures stability regions are plotted for values of charge parameter $s_1 = 0, 7.5, 14.5$ with R_c represented by "$\diamond$", "o" and "$*$" for $s_1 = 0.0$, $s_1 = 7.5$ and $s_1 = 14.5$, respectively. We observe that the value of R_c decreases as electromagnetic field increases, which are given in Tables **2-4** for different values of parameters. Figures **3-8** shows that cracking take place in each case for different values of the parameters corresponding to $s_1 = 7.5$ and $s_1 = 14.5$ in the quadratic regime, while remains stable in the absence of charge ($s_1 = 0.0$).

It is noted that the local DP scheme does not affect the stability of CO (remains stable) in neutral case, while change its stability (potentially unstable) drastically with the inclusion of charge in quadratic regime. Thus, the local DP scheme under nonlinear EoS considerably effect the stability regions of CO. When physical parameters like mass, electromagnetic field and density of anisotropic charged self-gravitating CO are locally perturbed, they drastically affect the sensitivity of radial forces which may leads towards the gravitational collapse. Therefore, the stability region of PSR J1614-2230 increases as value of electromagnetic field increases. Hence, we conclude that the binding forces of neutron star PSR J1614-2230 become stronger as we

move towards center of star and it becomes more dense as charge increases.

It is important to mentioned here that the idea of cracking was presented by Herrera [5] to understand the behavior of inner fluid distribution just after departure from equilibrium state may be responsible for cracking (overturning) of anisotropic sphere [8]. In his study, the global DP affects physical quantities like mass, tangential and radial pressure but do not effect pressure gradient. In this work global DP technique is modified by local density perturbations to study cracking in the presence of electromagnetic field. Finally, we conclude that the the given object exhibits cracking in the presence of electromagnetic field.

References

[1] Kausar, H. R. and Noureen, I.: Eur. Phys. J. C **74**(2014)2760.

[2] Joshi, P. S., Malafarina, D.: Int. J. Mod. Phys. D **20**(2011)2641.

[3] Bondi, H.: Proc. R. Soc. Lond. A **282**(1964)303.

[4] Chandrasekhar, S.: Phys. Rev. Lett. **12**(1964)114.

[5] Herrera, L.: Phys. Lett. A **165**(1992)206.

[6] Herrera, L. and Santos, N. O: Phys. Rep. **286**(1997)53.

[7] Herrera, L. and Varela, V.: Phys. Lett. A **226**(1997)143.

[8] Di Prisco, A., Fuenmayor, E., Herrera, L. and Varela, V.: Phys. Lett. A **195**(1994)23.

[9] Di Prisco, A., Herrera, L. and Varela, V.: Gen. Rel. Grav. **29**(1997)1239.

[10] Abreu, H., Hernandez, H. and Nunez, L.A.: Class. Quant. Grav. **24**(2007)4631.

[11] Gonzalez, G.A., Navarro, A. and Nunez, L.A.: arXiv: 1410.7733 (2014)

[12] Gonzalez, G.A., Navarro, A. and Nunez, L.A.: J. Phys. Conf. Ser. **600**, 012014 (2015)

[13] Bonnor, W.B.: Zeit. Phys. **160**(1960)59.

[14] Bonnor, W.B.: Mon. Not. R. Astron. Soc. **129**(1964)443.

[15] Bondi, H.: Proc. R. Soc. Lond. A **281**(1964)39.

[16] Bekenstein, J.D.: Phys. Rev. D **4**(1960)2185.

[17] Ray, S., Malheiro, M., Lemos, J.P.S. and Zanchin, V.T. : Braz. J. Phys. **34**(2004)310.

[18] Sharif, M. and Abbas, G.: Chin. Phys. B **22**(2013)030401.

[19] Sharif, M. and Azam, M.: Gen. Rel. Grav. **46**(2014)1647.

[20] Sharif, M. and Azam, M.: Chin. Phys. B **22**(2013)050401.

[21] Sharif, M. and Azam, M.: Eur. Phys. J. C **73**(2013)2407.

[22] Demorest, P.B., Pennucci, T., Ransom, S., Roberts, M.S.E. and Hessels, J.W.T.: Nature **467**(2010)1081.

[23] Tauris, T.M., Langer, N. and Kramer, M.: Mon. Not. R. Astron. Soc. **416**(2011)2130.

[24] Jinrong, L., Rappaport, S., Podsiadlowski, Ph., Nelson, L., Paxton, B. and Todorov, P.: ApJ. **732**(2011)70.

[25] Takisa, P.M., Maharaj, S.D. and Ray, S.: Astrophys. Space Sci. **354**(2014)463.

[26] Azam, M., Mardan, S.A. and Rehman, M.A.: Astrophys. Space Sci. **358**(2015)6, ibid. **359**(2015)14.

[27] Hansraj, S., Maharaj, S. D. and Mthethwa, T.: PRAMANA J. Phys. **81**(2013)557.